

FEDSM-ICNMM2010-' \$(*)

OPTICALLY INDUCED ELECTROKINETIC TRAPPING AND SORTING OF COLLOIDS

Stuart J. WILLIAMS¹, Alope KUMAR², Steven T. WERELEY²,

¹University of Louisville, Mechanical Engineering, Louisville, Kentucky, 40292, United States

²Purdue University, Birck Nanotechnology Center, West Lafayette, Indiana, 47907, United States

ABSTRACT

Recently, we have demonstrated electrothermal hydrodynamics with an external heating source of a highly focused 1,064 nm laser beam [1]. This phenomenon, when coupled with particle-electrode electrokinetic interactions, has led to the rapid and selective concentration of suspended colloids [2-6]. This technique, termed Rapid Electrokinetic Patterning (REP) was demonstrated without any additional surface modification or patterning of the electrodes. This dynamic, optically induced fluid and particle manipulation technique could be used for a variety of lab-on-a-chip applications. However, there are additional effects that have yet to be investigated that are important for a complete understanding of REP. This paper showcases experimental particle-particle behavior observations by varying particle diameter, electrode material, and preliminary results of varying fluid electrical conductivity.

INTRODUCTION

The ability to control the arrangement of micro- and nanoparticles is important in developing colloidal assembly methods at this scale. Nanomanufacturing is the 1D, 2D, or 3D construction of devices with nanometer resolution, and it is estimated that by 2015 there will be \$1T market incorporating nanomanufactured products [7]. The rapid and precise assembly of colloids is important for the advancement of similar nanomanufacturing techniques. One specific example of a product made from colloidal assembly is photonic crystals [8].

The optically induced electrokinetic technique described herein has distinct advantages over current methods like optical trapping [9, 10] and dielectrophoresis [11, 12]. This technique, termed Rapid Electrokinetic Patterning (REP), has demonstrated rapid, larger-scale close-packed assembly of

colloids. REP utilizes optically induced heating to create electrothermal fluid motion [1]. This electrohydrodynamic flow coupled with additional particle-particle and particle-electrode interactions results in the capture hundreds of colloids suspended in an aqueous solution (Figure 1.). REP is optically-induced, offering dynamic control over the location and shape of the particle aggregation. REP has concentrated and manipulated polystyrene, latex, and silica particles (49 nm to 3.0 μm) at applied AC signals 1 kHz-150 kHz and 0-20 volts peak-to-peak (V_{pp}) with near-infrared illuminations (1,064 nm) under 100 mW [2-6].

Three AC electrokinetic phenomena are the primary mechanisms responsible for the continuous concentration of particles. First, a microfluidic vortex is generated from optically induced electrothermal fluid motion. Optically induced electrothermal hydrodynamics have been investigated previously with laser [13] and broad illumination sources [14]. The resulting microfluidic vortex within REP was used to expedite particle concentration. As a particle is carried towards the surface of the electrode low frequency (20 kHz - 200 kHz) particle-electrode electrokinetic forces trap the particle onto the electrode surface [15-18]. As the frequency is increased, particles are released yet continue to circulate within the microfluidic vortex. The maximum particle trapping frequency is a function of medium conductivity and particle type and size.

Previous REP investigations have demonstrated that the maximum trapping frequency of similar particles is inversely proportional to the square of the particle radius [5, 6]. Mobile ions within the double layer take a finite amount of time to polarize the particle. Therefore at higher frequencies a particle will be unable to polarize and will no longer be captured. This dispersion occurs at frequencies lower than the Maxwell-Wagner interfacial polarization [19-21] and its relaxation

frequency is proportional to the particle's surface area (radius squared).

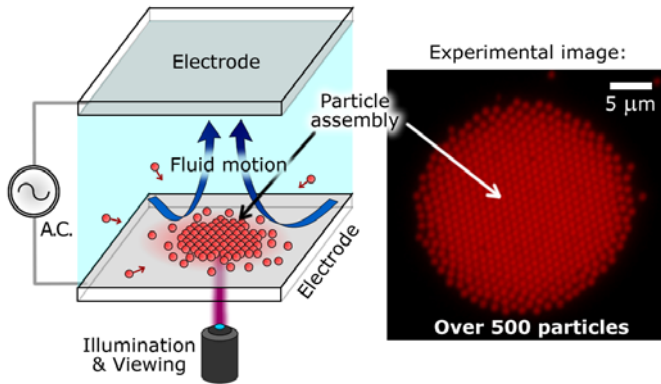


Figure 1. A highly focused laser beam (1,064 nm) is focused onto one surface of the parallel plate electrodes. The electric field acts upon the optically induced thermal gradients, resulting in a microfluidic vortex. At low AC frequencies, the vortex carries particles to the surface of the electrode where they aggregate. Shown are 1.0 μm particles captured with REP. From [6].

The electrokinetic motion and interaction of neighboring particles on the surface of an electrode with [5] and without [22-26] REP have also been investigated. Particle-particle interactions include dipole-dipole repulsive forces, localized AC electro-osmotic attractive forces, inward fluid drag from the microfluidic vortex, and other electrokinetic phenomena. These electrokinetic mechanisms are complex and are not completely understood. These forces are a function of AC frequency, electric field magnitude, particle size, electrolyte conductivity, and electrolyte type. This manuscript further investigates these particle-particle interactions within the compact aggregation and characterizes particle-particle distance as a function of voltage, frequency, and fluid conductivity.

EXPERIMENTAL

The testing chip consists of a microfluidic chamber between two parallel-plate electrodes. One plate was an indium tin oxide (ITO) coated glass cover slip (170 μm thick) and the opposite electrode was a thicker ITO-coated glass piece (0.7 mm thick). In some experiments a gold-coated microscope slide (0.7 mm thick) was used instead of the thicker ITO piece. A 50 μm thick, double-sided adhesive tape contained microfluidic features and separated the parallel electrodes. The experimental area was far from microchannel side walls to ensure a uniform electric field.

An inverted Nikon TE2000U microscope was equipped with a Nikon 40X water-immersion lens (0.8 N.A. and 2.0 mm working distance). The laser illumination source was a Nd:YAG laser-based holographic illumination system (Bioryx® 200 from Arryx Inc., Chicago, USA) operating at 1,064 nm. Although complicated holographic optical

landscapes could be incorporated [10] to pattern colloidal aggregations [4], only a single focused beam of light was used in these experiments. All stated experimental illumination intensities were with respect to the measured illumination intensity immediately before the objective lens.

Carboxylate-modified fluorescent polystyrene particles (1.0 μm , 2.0 μm , Invitrogen, OR, USA) were used for observations of particle-particle interactions within REP. The concentration of suspended colloids remained constant throughout all experiments. The medium was prepared by diluting 50 μL of a 2% solids particle solution with 10 mL of an aqueous solution of potassium chloride (KCl) with a conductivity of 1.5 mS/m, 2.4 mS/m, or 4.1 mS/m.

Images of the captured colloids were acquired with an interline transfer charge coupled device (CCD) camera (Coolsnap HQ, Photometrics, Roper Scientific Inc.). Images were processed by a MATLAB program that determined the number of acquired particles as well as their particle-particle distance.

RESULTS

A critical element in REP is the optically induced heating and subsequent electrothermal microfluidic vortex. REP has been demonstrated with 1,064 nm illumination heating an ITO- and gold-coated glass slide. The liquid is heated from the optically heated substrate. Alternatively, the liquid could be heated by the illumination directly with infrared illumination; for example, water absorbs 1,550 nm illumination 71 times more than at 1,064 nm [27]. In addition, the optical absorption of electrode materials is a function of the wavelength of illumination. For example, ITO absorbs infrared more readily than visible light. The reflectance of gold at 1,064 nm, 532 nm, and 400 nm is approximately 0.99, 0.7, and 0.37, respectively [27].

A comparison between the heating of ITO, gold, and plain glass substrates was explored previously [5] using laser induced fluorescence [28]. The maximum observed heating for each substrate is illustrated in Figure 2. The 1,064 nm laser heated the ITO cover slip over four times more than the gold coated microscope slide and approximately 40 times more than the glass cover slip. The 1,064 nm illumination is more likely to heat the liquid (water) than the plain glass cover slip since the transmittance of typical commercially available glasses is greater than 0.99 [27]. The measured optical heating of the glass cover slip (~ 0.5 $^{\circ}\text{C}$ per 100 mW) was less than the rate of heating water with 1,064 nm optical tweezers [29] of approximately 1.5 $^{\circ}\text{C}$ per 100 mW. Taking into account the measurement error of this technique [28], these measurements were found to be comparable to those in literature.

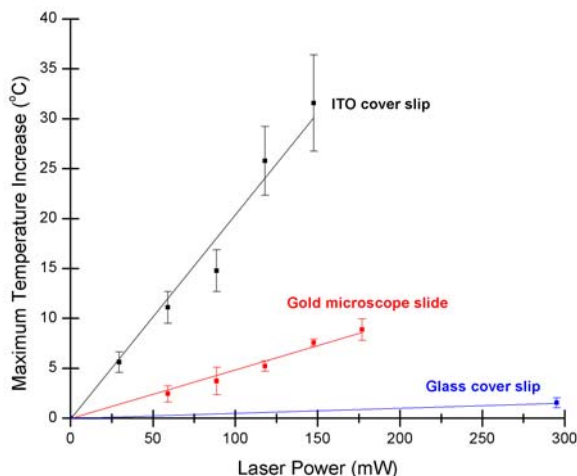


Figure 2. Maximum observed heating of a substrate with 1,064 nm illumination at various applied laser intensities. From [5].

When 1,064 nm illumination was focused on the surface of an ITO electrode, the microfluidic vortex was directed inward as expected from previous results (Fig. 3a). This was observed on either surface of an ITO/ITO chip with a variety of lens magnifications (20X, 40X, 60X, 100X). Inward vortex motion on both surfaces of an Au/ITO chip occurred with lens magnifications of 60X and 100X (Fig. 3.3b). With the same Au/ITO chip and a 40X lens, the vortex direction was outward on the gold surface despite flowing inward when the illumination was focused on the ITO surface (Fig. 3.3c). This reversal in fluid motion on the gold surface was due to the dominant optically induced heat on the opposite ITO cover slip. For this scenario the thermal gradients on the ITO surface was still greater, although the laser was focused on the gold surface with a 40X lens. The electrode surface experiencing greater heating controlled the overall direction of the vortex. At higher magnifications (> 40X), the temperature of the opposing ITO electrode was reduced due to the greater divergence of the laser beam, and therefore heating of the gold surface dominated. The numerical aperture (NA) of the 40X, 60X, and 100X lenses were 0.8, 1.2, and 1.3 respectively. Assuming an index of refraction of 1.33 (water), numerical apertures correspond to a divergence half angle of 37°, 64°, and 78°, respectively. Substantial heating of the opposite ITO surface was prevented using the greater beam divergence with the 60X and 100X lenses, allowing particles to be captured on the gold surface.

Unfortunately, temperature measurements could not be provided to compare simultaneous temperature profiles on opposing surfaces with temperature dependent fluorescent dye. Measurements were restricted to the observation plane only, which was the same as the illumination focal plane. From these observations it is important that the optically induced heating on both substrates needs to be considered for the future designs of REP systems.

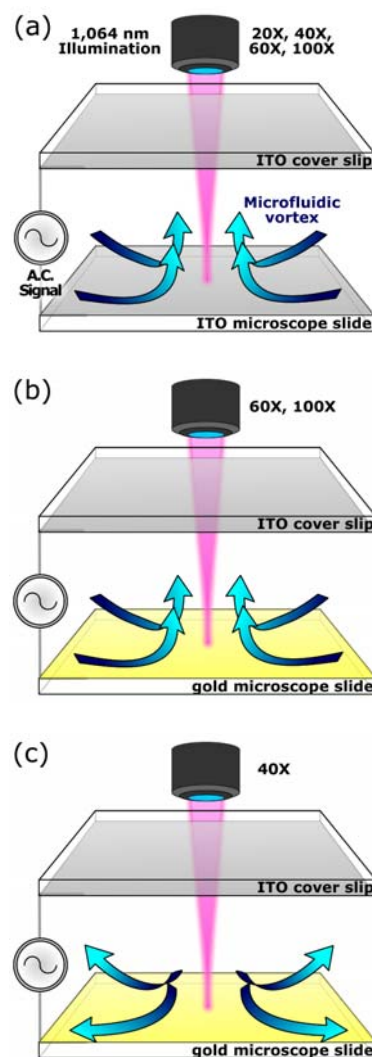


Figure 3. The observed direction of the microfluidic vortex motion for (a) ITO/ITO chip, (b) Au/ITO chip with 60X and 100X lenses, and (c) Au/ITO chip with a 40X lens.

A practical step would be to create an inexpensive system capable of inducing REP. Recent REP experimentations have been limited to using an expensive holographic optical trapping systems costing over \$100,000. REP is not restricted to one particular illumination wavelength or electrode material. Thermal gradients necessary for REP can be created by properly coupling the wavelength of the focused illumination with substrates and/or electrode materials. REP could be induced with alternative illumination components such as laser diodes. REP on a gold surface was successful at 532 nm and also at 1,064 nm with 60X (1.2 NA) and 100X (1.3 NA) objective lenses. Therefore a low cost, portable REP system utilizing laser diode technology seems feasible.

Particle-particle interactions within the REP aggregation can be controlled for precise colloidal arrangements or

advanced particle sorting. For particles greater than 0.5 μm in diameter, REP typically produces a crystalline-like monolayer of colloidal aggregations. In prior experiments, it was observed that particle-particle distance within an aggregation changed as a function of frequency. Frequency dependent particle-particle distances were investigated as a function of (i) voltage, (ii) fluid conductivity, and (iii) particle diameter. REP can be used to investigate particle-particle electrokinetic forces by examining particle positions within the aggregation. In most cases the range of capturing frequencies is less than the charge relaxation frequency of the fluid, resulting in constant vortex fluid velocities. The following results are preliminary and require additional in-depth investigations to fully understand electrokinetic interactions.

After image acquisition, a MATLAB program determined individual particle centers with sub-pixel accuracy. For each particle, center-to-center distances between it and its closest three neighbors were determined. The total number of data points was three times the number of detected particles. One-fifth of the largest and smallest particle-particle distances (10% each) were omitted to remove erroneous data. The data was presented in terms of a non-dimensional term, λ_p , which is the center-to-center particle distance divided by the particle diameter. Fluorescent 1.0 μm carboxylate modified polystyrene beads were used to analyze particle distance as a function of voltage and fluid conductivity. Fluorescent 2.0 μm carboxylate modified beads were used to explore λ_p as a function of particle diameter.

Two sample images of 1.0 μm particle aggregations are demonstrated in Figure 4 at (a) 100 kHz and (b) 60 kHz at 23 mW, 1.5 mS/m, and 17.5 V_{pp} . There was a distinct difference in the distance between neighboring particles at various frequencies. It was also observed that the particles on the perimeter of the aggregation were spaced further apart from their neighbors. This is explained by the decreasing radial component of fluid velocity as the distance from the microfluidic vortex's center increases.

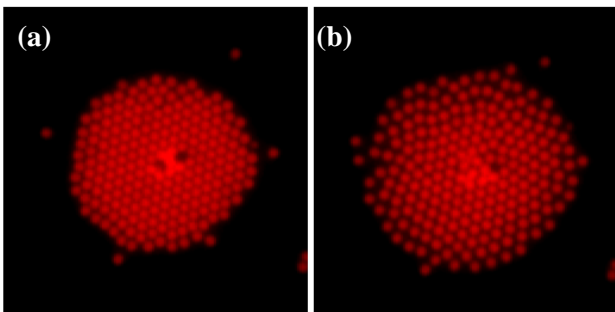


Figure 4. Experimental images of the particle-particle distance for applied frequencies of (a) 100 kHz and (b) 60 kHz at 23 mW, 1.5 mS/m, and 17.5 V_{pp} .

Polystyrene 1.0 μm beads were used to analyze particle-particle distance as a function of voltage at constant illumination (25 mW) and fluid conductivity (2.4 mS/m). The results for three applied voltages (15.3 V_{pp} , 17.3 V_{pp} , and 19.2 V_{pp}) are demonstrated in Figure 5. Error bars from measurements were omitted for clarity. One standard deviation of λ_p for each point was approximately 0.1. The results revealed that the particle-particle distance was independent of voltage at this range. Theories describing the electrothermal fluid velocity, dipole-dipole repulsive force, and attractive particle-particle electrohydrodynamics all scale with the square of the applied electric field (E^2). As these forces scale at the same rate, the particle-particle distance remain unaffected as a function of voltage for static particles. Also, there exists a frequency at which λ_p reached a minimum, which was approximately 78 kHz \pm 10 kHz (\pm one standard deviation) for these voltages.

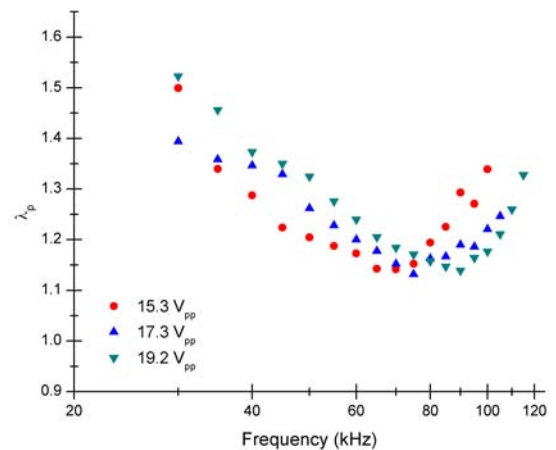


Figure 5. Particle-particle distance of 1.0 μm beads as a function of frequency for various voltages at constant illumination (25 mW) and fluid conductivity (2.4 mS/m).

Results plotted in Figure 6 examine the particle-particle distance of 1.0 μm beads as a function of medium conductivity. Particle interaction was strongly dependent upon on fluid conductivity. The arrows in Figure 6 depict the frequency at which minimum particle-particle distance occurred. As fluid conductivity increased the frequency of minimum λ_p decreased. According to Mittal et al. [30], the dipole-dipole repulsive force decreased with increased conductivity. The relationship between the frequency of minimum λ_p and conductivity appeared to be inversely proportional to each other. Previous experiments determined that hydrodynamic drag exerted on the particles remained constant for frequencies lower than its charge relaxation [1]. The charge relaxation frequencies for 1.5 mS/m, 2.4 mS/m, and 4.1 mS/m are 340 kHz, 540 kHz, and 920 kHz, respectively. Assuming the hydrodynamic drag exerted on the particle group was constant for these experiments, the change in particle-particle spacing was

governed by local electrokinetic and electrohydrodynamic forces.

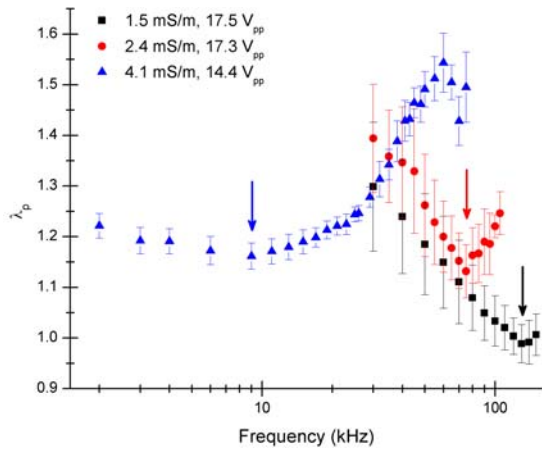


Figure 6. Particle-particle distance of 1.0 μm beads as a function of frequency for varied fluid conductivities. The minima of λ_p for each conductivity are labeled with arrows. Error bars represent two standard deviations.

Literature hypothesized both frequency and particle-particle distance dependence on particle-induced electrohydrodynamic flow [31, 32]. This included theories on flow reversal [33]; however, extensive experimental confirmation of such models do not exist. An observed trend throughout literature was that particles on an electrode surface disaggregate at larger frequencies [24, 25]. Local electrohydrodynamic fluid velocity was inversely proportional with applied frequency. This trend explains the observed increase in λ_p at higher frequencies, yet this conclusion does not account for the increase in particle-particle distance for lower frequencies. An increase in particle-particle distance with decreasing frequencies could be explained by electrohydrodynamic flow reversal or an increase in particle polarization. With larger polarization, the electrokinetic repelling force is stronger.

Frequency dependent particle-particle interactions at present cannot be fully explained, REP lends itself as a valuable tool to investigate low-frequency polarization mechanisms and particle-induced electrohydrodynamics, given that the applied microvortex fluid drag was constant within the AC frequency range of interest.

Next, carboxylate modified particles 1.0 μm and 2.0 μm in diameter were introduced at constant voltage (14.4 V_{pp}), fluid conductivity (4.1 mS/m), and applied illumination (25 mW). Larger 2.0 μm particles reached their minimum particle-particle distance at a lower frequency as compared to the smaller 1.0 μm particles (Fig. 7). This was anticipated as larger particles faced greater dipole-dipole repulsive forces, which scale with particle radius to a power of six. An expanded range of particle diameters should be experimented to confirm theoretical

electrokinetic trends. Carboxylate modified particles greater than 2.0 μm were not available and those less than 1.0 μm formed two (or more) layers of particles serving to complicate this analytical procedure.

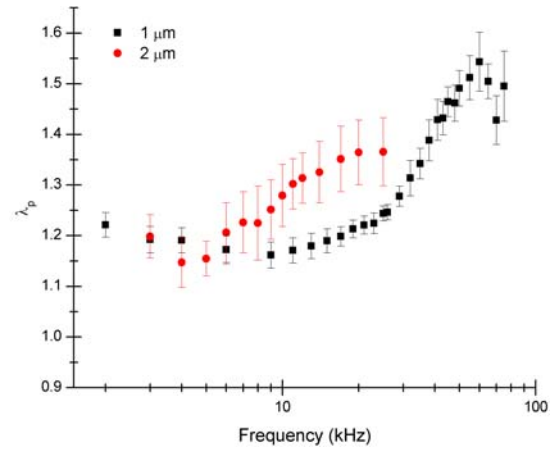


Figure 7. Frequency dependent particle-particle distance for 1.0 μm and 2.0 μm beads with all other parameters held constant. Error bars represent two standard deviations.

It was observed during particle concentration experiments that smaller particle aggregations tend to form multiple layers whereas particles greater than 1.0 μm in diameter remain arranged as a monolayer. For instance, nanoparticle aggregation [3] was visualized as a Gaussian-shaped fluorescent spot. The initial formation of multiple layers was observed with 0.5 μm and 0.69 μm diameter polystyrene particles. Figure 8 shows an aggregation of 0.5 μm particles suspended in a 4.1 mS/m solution captured at 50 kHz and 13 V_{pp} . A small number of particles within the aggregation formed a second layer of particles. These particles were located above a junction where three underlying particles met. This four particle arrangement formed a tetrahedron structure. When illumination was deactivated, the particle aggregation scattered as anticipated [5, 6] however some of these tetrahedron structures remained intact. Multiple tetrahedrons and multiple particle layers were inclined to form at greater particle concentrations and higher voltages. Future research will continue to explore the physics behind the creation of multiple layers and these tetrahedron structures. This concept could be used to create numerous multi-particle or multi-layered structures. Future research includes varying particle diameter and particle types in order to enable the creation of precisely tuned artificial architectures such as colloidal crystals.

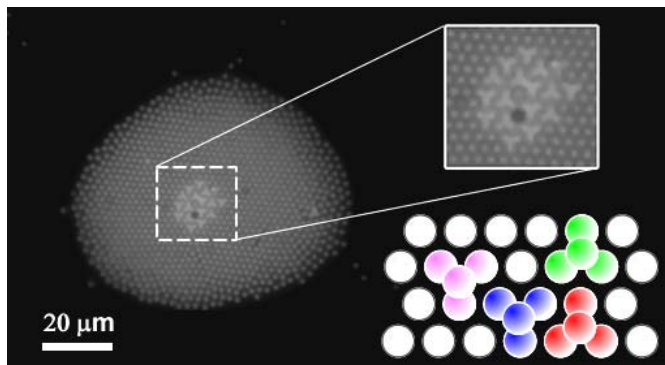


Figure 8. An aggregation of 0.5 μm particles at 4.1 mS/m, 13 V_{pp} , and 50 kHz. A second layer of particles occurred within the aggregation, creating tetrahedron particle formations. Their arrangement is also illustrated (lower-right).

CONCLUSIONS

REP has been shown to dynamically, rapidly, and continuously concentrate, translate, sort, and pattern colloids [2-6]. However, additional experiments are necessary to completely understand the physics involved with REP such to optimize any colloidal assembly process which will aid in manufacturing processes at this scale. This manuscript demonstrated preliminary results showcasing electrokinetic particle-particle interactions within a colloidal aggregation with simultaneous electrothermal fluid motion. These interactions are rather complex involving fluid dynamics, particle-particle electrokinetic mechanisms, and particle-electrode interactions. Future experiments will expand upon these findings in order to precisely tune and optimize REP colloidal assembly. In general, REP is a versatile tool that can be applied to variety of existing lab-on-a-chip techniques.

REFERENCES

1. Kumar, A., S.J. Williams, and S.T. Wereley, "Experiments on opto-electrically generated microfluidic vortices," *Microfluidics and Nanofluidics*, 2009. **6**, 637-646.
2. Williams, S.J., A. Kumar, and S.T. Wereley, "Electrokinetic patterning of colloidal particles with optical landscapes," *Lab on a Chip*, 2008. **8**, 1879-1882.
3. Williams, S.J., A. Kumar, and S.T. Wereley, "A simple, optically induced electrokinetic method to concentrate and pattern nanoparticles," *Nanoscale*, 2009. **1**, 133-137.
4. Williams, S.J., A. Kumar, and S.T. Wereley. *Optically induced electrokinetic patterning and manipulation of particles*. APS DFD Gallery of Fluid Motion [Video] 2008 [cited; Available from: <http://hdl.handle.net/1813/11399>].
5. Kumar, A., J.-S. Kwon, S.J. Williams, N.G. Green, N.K. Yip, and S.T. Wereley, "Optically modulated electrokinetic manipulation and concentration of colloidal particles near an electrode surface," *Langmuir*, 2010. **26**, 5262-5272.
6. Williams, S.J., A. Kumar, N.G. Green, and S.T. Wereley, "Optically induced electrokinetic concentration and separation of

colloids," *Journal of Micromechanics and Microengineering*, 2010. **20**.

7. Roco, M.C. and W.S. Bainbridge, *Societal Implications of Nanoscience and Nanotechnology*. 1 ed. 2001: Springer.
8. Noda, S., T. Baba, and Optoelectronic Industry and Technology Development Association (Japan), *Roadmap on photonic crystals*. 2003, Dordrecht ; Boston: Kluwer Academic Publishers.
9. Curtis, J.E., B.A. Koss, and D.G. Grier, "Dynamic holographic optical tweezers," *Optics Communications*, 2002. **207**, 169-175.
10. Grier, D.G., "A revolution in optical manipulation," *Nature*, 2003. **424**, 810-816.
11. Morgan, H. and N.G. Green, *AC electrokinetics : colloids and nanoparticles*. Microtechnologies and microsystems series ; 2. 2003, Philadelphia, PA: Research Studies Press.
12. Chiou, P.Y., A.T. Ohta, and M.C. Wu, "Massively parallel manipulation of single cells and microparticles using optical images," *Nature*, 2005. **436**, 370-372.
13. Mizuno, A., M. Nishioka, Y. Ohno, and L.D. Dascalescu, "Liquid Microvortex Generated around a Laser Focal Point in an Intense High-Frequency Electric-Field," *IEEE Transactions on Industry Applications*, 1995. **31**, 464-468.
14. Green, N.G., A. Ramos, A. Gonzalez, A. Castellanos, and H. Morgan, "Electric field induced fluid flow on microelectrodes: the effect of illumination," *Journal of Physics D-Applied Physics*, 2000. **33**, L13-L17.
15. Fagan, J.A., P.J. Sides, and D.C. Prieve, "Vertical motion of a charged colloidal particle near an AC polarized electrode with a nonuniform potential distribution: Theory and experimental evidence," *Langmuir*, 2004. **20**, 4823-4834.
16. Fagan, J.A., P.J. Sides, and D.C. Prieve, "Evidence of multiple electrohydrodynamic forces acting on a colloidal particle near an electrode due to an alternating current electric field," *Langmuir*, 2005. **21**, 1784-1794.
17. Fagan, J.A., P.J. Sides, and D.C. Prieve, "Vertical oscillatory motion of a single colloidal particle adjacent to an electrode in an ac electric field," *Langmuir*, 2002. **18**, 7810-7820.
18. Yeh, S.R., M. Seul, and B.I. Shraiman, "Assembly of ordered colloidal aggregates by electric-field-induced fluid flow," *Nature*, 1997. **386**, 57-59.
19. Green, N.G. and H. Morgan, "Dielectrophoresis of submicrometer latex spheres. 1. Experimental results," *Journal of Physical Chemistry B*, 1999. **103**, 41-50.
20. Schwan, H.P., G. Schwarz, J. Maczuk, and H. Pauly, "On Low-Frequency Dielectric Dispersion of Colloidal Particles in Electrolyte Solution," *Journal of Physical Chemistry*, 1962. **66**, 2626-&.
21. Schwarz, G., "A Theory of Low-Frequency Dielectric Dispersion of Colloidal Particles in Electrolyte Solution," *Journal of Physical Chemistry*, 1962. **66**, 2636.
22. Hoggard, J.D., P.J. Sides, and D.C. Prieve, "Electrolyte-dependent multiparticle motion near electrodes in oscillating electric fields," *Langmuir*, 2008. **24**, 2977-2982.
23. Liu, Y., R.G. Xie, and X.Y. Liu, "Fine tuning of equilibrium distance of two-dimensional colloidal assembly under an alternating electric field," *Applied Physics Letters*, 2007. **91**.
24. Nadal, F., F. Argoul, P. Hanusse, B. Pouligny, and A. Ajdari, "Electrically induced interactions between colloidal particles in the vicinity of a conducting plane," *Physical Review E*, 2002. **65**, 8.

25. Ristenpart, W.D., I.A. Aksay, and D.A. Saville, "Assembly of colloidal aggregates by electrohydrodynamic flow: Kinetic experiments and scaling analysis," *Physical Review E*, 2004. **69**.
26. Santana-Solano, J., D.T. Wu, and D.W.M. Marr, "Direct measurement of colloidal particle rotation and field dependence in alternating current electrohydrodynamic flows," *Langmuir*, 2006. **22**, 5932-5936.
27. Weber, M.J., *Handbook of Optical Materials*. 2003, Boca Raton: CRC Press.
28. Williams, S.J., P. Chamarthy, and S.T. Wereley, "Comparison of experiments and simulation of Joule heating in AC electrokinetic chips," *Journal of Fluids Engineering*, 2010. **132**, 021103.
29. Mao, H.B., J.R. Arias-Gonzalez, S.B. Smith, I. Tinoco, and C. Bustamante, "Temperature control methods in a laser tweezers system," *Biophysical Journal*, 2005. **89**, 1308-1316.
30. Mittal, M., P.P. Lele, E.W. Kaler, and E.M. Furst, "Polarization and interactions of colloidal particles in ac electric fields," *The Journal of Chemical Physics*, 2008. **129**, 064513.
31. Ristenpart, W.D., I.A. Aksay, and D.A. Saville, "Electrohydrodynamic flow around a colloidal particle near an electrode with an oscillating potential," *Journal of Fluid Mechanics*, 2007. **575**, 83-109.
32. Ristenpart, W.D., I.A. Aksay, and D.A. Saville, "Electrically driven flow near a colloidal particle close to an electrode with a faradaic current," *Langmuir*, 2007. **23**, 4071-4080.
33. Sides, P.J., "Calculation of electrohydrodynamic flow around a single particle on an electrode," *Langmuir*, 2003. **19**, 2745-2751.